MOLECULAR AND CELLULAR BIOLOGY, Sept. 2006, p. 6333–6346 Vol. 26, No. 17
0270-7306/06/$08.00+0 doi:10.1128/MCB.00207-06

Exchange Protein Activated by Cyclic AMP (Epac)-Mediated Induction of Suppressor of Cytokine Signaling 3 (SOCS-3) in Vascular Endothelial Cells

William A. Sands, Hayley D. Woolson, Gillian R. Milne, Claire Rutherford, and Timothy M. Palmer*

Molecular Pharmacology Group, Division of Biochemistry and Molecular Biology, Institute of Biomedical and Life Sciences, University of Glasgow, Glasgow G12 8QQ, United Kingdom

Received 6 February 2006/Returned for modification 28 March 2006/Accepted 8 June 2006

Here, we demonstrate that elevation of intracellular cyclic AMP (cAMP) in vascular endothelial cells (ECs) by either a direct activator of adenylyl cyclase or endogenous cAMP-mobilizing G protein-coupled receptors inhibited the tyrosine phosphorylation of STAT proteins by an interleukin 6 (IL-6) receptor *trans*-signaling complex (soluble IL-6Rα/IL-6). This was associated with the induction of suppressor of cytokine signaling 3 (SOCS-3), a bona fide inhibitor in vivo of gp130, the signal-transducing component of the IL-6 receptor complex. Attenuation of SOCS-3 induction in either ECs or SOCS-3-null murine embryonic fibroblasts abolished the inhibitory effect of cAMP, whereas inhibition of SHP-2, another negative regulator of gp130, was without effect. Interestingly, the inhibition of STAT phosphorylation and SOCS-3 induction did not require cAMP-dependent protein kinase activity but could be recapitulated upon selective activation of the alternative cAMP sensor Epac, a guanine nucleotide exchange factor for Rap1. Consistent with this hypothesis, small interfering RNA-mediated knockdown of Epac1 was sufficient to attenuate both cAMP-mediated SOCS-3 induction and inhibition of STAT phosphorylation, suggesting that Epac activation is both necessary and sufficient to observe these effects. Together, these data argue for the existence of a novel cAMP/Epac/Rap1/SOCS-3 pathway for limiting IL-6 receptor signaling in ECs and illuminate a new mechanism by which cAMP may mediate its potent anti-inflammatory effects.

Vascular endothelial cells (ECs) represent a major cellular target for many pro- and anti-inflammatory cytokines. Some of the most important are class I cytokines, including the adipocytokine leptin and "interleukin 6 (IL-6) family" members such as IL-11, oncostatin M, and prototypical member IL-6 (19). Activated vascular ECs, smooth muscle cells, monocytes, and macrophages are each capable of producing IL-6, and accumulation of IL-6 has been noted within arterial lesions in several models of atherosclerosis (42, 54). Responsiveness to IL-6 requires two components: an IL-6 α-receptor (IL-6Rα) which binds the cytokine with high affinity, and gp130, which cannot bind IL-6 directly but can interact with IL-6-bound IL-6Rα to transduce an intracellular signal (19). While the endothelium is unresponsive to IL-6 alone due to a lack of endogenous IL-6Rα, soluble IL-6Rα (sIL-6Rα) derived from hepatocytes or shed from monocytes and macrophages recruited to sites of vascular injury can bind IL-6 to form a sIL-6Rα/IL-6 so-called "*trans*-signaling" complex that can interact with and activate gp130 homodimers (30). This has been reported to trigger the initiation of angiogenesis, the up-regulation of adhesion molecules, such as E-selectin, ICAM-1 and VCAM-1, and the accumulation of chemokines such as monocyte chemoattractant protein-1 (MCP-1/CCL2) (19, 22, 37). In contrast, adipocyte-derived leptin can directly bind and activate any of several splice variants of the leptin receptor Ob-R, although ECs appear to express only the full-length Ob-Rb isoform (58).

Signaling from both gp130 and Ob-Rb is initiated upon receptor clustering and subsequent activation of receptor-associated "Janus kinases" (JAKs), which catalyze the phosphorylation of each receptor on specific Tyr residues within their cytoplasmic domains. This triggers recruitment of members of the "signal transducers and activators of transcription" (STAT) family and their subsequent phosphorylation by JAKs. Upon Tyr phosphorylation, STATs dissociate from the receptors to form either homo- or heterodimeric complexes that translocate to the nucleus to initiate target gene transcription upon binding specific DNA elements and recruiting transcriptional coactivators. The protein Tyr phosphatase "*SH*2 domain-containing protein tyrosine *p*hosphatase 2" (SHP-2) also binds to specific phospho-Tyr residues within gp130 and Ob-Rb, thereby mediating the recruitment of Grb2-Sos complexes that initiate the Ras/Raf/mitogen-activated protein kinase-ERK kinase (MEK)/extracellular signal-related kinase (ERK) signaling cascade (19, 58).

Signaling from cytokine receptors is subject to strict negative regulation via several mechanisms designed to prevent inappropriately sustained activation of downstream responses (55). For example, the transcriptional activity of phosphorylated STAT proteins can be inhibited via SUMOylation by PIAS proteins ("protein inhibitors of activated STATs") or by targeting for proteasomal degradation via ubiquitylation by E3 ligases, such as SLIM (36, 52). Also, in addition to initiating the ERK pathway, SHP-2 is capable of inhibiting downstream signaling by dephosphorylating Tyr phosphorylated cytokine receptors, JAKs, and STATs (19, 55). However, one of the

* Corresponding author. Mailing address: 425 Davidson Bldg., Molecular Pharmacology Group, Division of Biochemistry and Molecular Biology, Institute of Biomedical and Life Sciences, University of Glasgow, Glasgow G12 8QQ, United Kingdom. Phone: 44 141 330 4626. Fax: 44 141 330 4620. E-mail: T.Palmer@bio.gla.ac.uk.

most important inhibitory mechanisms identified is the induction of "*s*uppressor *o*f *c*ytokine *s*ignaling" (SOCS) proteins. These constitute a family of eight related proteins (CIS and SOCS-1 to -7), of which SOCS-1 and SOCS-3 have been characterized most intensively, that function as end points in a classical negative feedback loop whereby activation of STATs triggers the induction of SOCS proteins, which then bind and terminate signaling from activated cytokine receptors (2, 27). A role for SOCS-3 in specifically terminating gp130 and Ob-Rb signaling has been demonstrated by several observations, including the unrestricted agonist-stimulated activation of STAT3 seen in macrophages, hepatocytes, and neurons from cell-specific conditional SOCS-3-deficient mice (8, 32, 56). SOCS-3 terminates signaling by binding to JAK-phosphorylated receptors via its SH2 domain and interacting with and inhibiting adjacent JAKs via its "kinase inhibitory region," thereby preventing the recruitment and Tyr phosphorylation of STATs (41). SOCS-3 can also potentially competitively block receptor recruitment of SHP-2 to Tyr759 of gp130, thus inhibiting ERK activation (43). In addition, the C-terminal "SOCS box" domain can target SH2 domain-bound partners for proteasomal degradation by directing interaction with an elongin B/C-Cul5-Rbx1 complex to form an E3 ubiquitin ligase (23, 38).

SOCS-1 and SOCS-3 can also be induced by noncytokine stimuli, thus providing a mechanism by which otherwise distinct signaling pathways can negatively control cytokine responsiveness. These include the chemokine IL-8 and bacterially derived chemoattractant formylmethionyl-leucyl-phenylalanine following activation of their cognate G protein-coupled receptors (50), and lipopolysaccharide (LPS) via Toll-like receptor 4 (51). One recently identified signal for SOCS induction is elevation of intracellular cyclic AMP (cAMP) (16, 34). The ability of this prototypical second messenger to suppress activation of the NF-κB pathway at several levels in many cell types has been the most intensively studied aspect of its anti-inflammatory effects (31). However, the induction of SOCS-1 and SOCS-3 observed in leukocytes and FRTL-5 thyroid cells suggests a potential mechanism by which cAMP could block pro-inflammatory signaling from multiple JAK-STAT-mobilizing cytokine receptors (16, 34). Classically, cAMP is thought to mediate the vast majority of its intracellular effects by binding and activating cAMP-dependent protein kinase (PKA), which controls the phosphorylation status and activity of multiple intracellular substrates (53). However, another family of intracellular cAMP sensors termed "*e*xchange *p*roteins directly *a*ctivated by *c*AMP" (Epacs) have been recently identified (10). Epac1 and -2 function as cAMP-activated guanine nucleotide exchange factors specific for the Rap family of small G proteins and, thus, promote the accumulation of active GTP-bound Rap1 and -2 (5, 10). Interestingly, a role for Epac in EC function was recently revealed by the finding that the Epac-mediated activation of Rap1 and the subsequent formation of adherens junctions contribute toward the ability of cAMP to enhance endothelial barrier function, an important aspect of its anti-inflammatory effects in vascular ECs (9, 15).

To begin identifying potential mechanisms by which cAMP could impact on cytokine signaling, we have been examining the effects of cAMP elevation on IL-6 receptor signaling in vascular ECs and assessing its functional significance. Our observations suggest that cAMP-mediated inhibition of IL-6 receptor signaling occurs independently of SHP-2 but requires induction of SOCS-3. Moreover, the induction of SOCS-3 and the subsequent inhibition of STAT phosphorylation occur independently of PKA, instead requiring Epac-mediated activation of Rap1.

MATERIALS AND METHODS

Materials. Recombinant human leptin, IL-6, and sIL-6Rα were obtained from R&D Systems Europe, Ltd. (Abingdon, United Kingdom). Forskolin, rolipram, H89, monoperoxo(picolinato)oxovanadate (mpV), U0126, polymyxin B, and JAK inhibitor I were obtained from Merck Biosciences (Nottingham, United Kingdom). Prostaglandin E_2 (PGE_2) and α-melanocyte-stimulating hormone (αMSH) were from Sigma-RBI (Dorset, United Kingdom). The Epac-selective activator 8-(4-chlorophenylthio)-2′-*O*-methyladenosine-3′,5′-cyclic monophosphate (8-pCPT) was from the Biolog Life Science Institute (Bremen, Germany). Human umbilical vein endothelial cells (HUVECs) and human aortic endothelial cells (HAECs) were purchased from Cambrex Biosciences Nottingham, Ltd. (Nottingham, United Kingdom). The MCP-1 sandwich enzyme-linked immunosorbent assay (ELISA) kit was from Promocell (Heidelberg, Germany). Endo-Porter delivery reagent and morpholino antisense oligonucleotides against SOCS-3 and C/EBPα were purchased from Gene Tools, LLC (Philomath, OR), while control nontargeting (catalog no. D-001210-0120) and Epac1-targeted (catalog no. M-007676-00) small interfering RNAs (siRNAs) were purchased from Dharmacon (Lafayette, CO). Wild-type (SOCS-$3^{+/+}$) and SOCS-$3^{-/-}$ murine embryonic fibroblasts (MEFs) were generously provided by Akihiko Yoshimura (Kyushu University, Japan), while functionally null SHP-$2^{\Delta 46\text{-}110}$ 3T3 fibroblasts and SHP-$2^{\Delta 46\text{-}110}$ cells in which function had been rescued by stable expression of full-length wild-type SHP-2 (59) (SHP-$2^{+/+}$ cells) were generously provided by Benjamin Neel (Beth Israel Deaconess Medical Center, Harvard Medical School, Boston, MA). Human SOCS-1 and SOCS-3 expression constructs were generously provided by Doug Hilton (Walter and Eliza Hall Institute for Medical Research and Co-operative Research Centre for Cellular Growth Factors, Parkville, Victoria, Australia) and Jim Johnston (Centre for Cancer Research and Cell Biology, Queen's University, Belfast, United Kingdom). Expression constructs encoding hemagglutinin-tagged Val12Rap1a and myc-tagged Leu61Cdc42 were generously donated by Johannes Bos (University Medical Center, Utrecht, Netherlands) and Martin Schwartz (Mellon Prostate Cancer Institute, University of Virginia, Charlottesville, VA), respectively. Antibodies were from Cell Signaling Technology, Inc. (Beverly, MA) except those against Epac1 (characterized in reference 26) (generously supplied by Johannes Bos), SOCS-1 and SOCS-3 (sc-7005 and sc-7009, respectively; Santa Cruz Biotechnology, Santa Cruz, CA), glyceraldehyde-3-phosphate dehydrogenase (GAPDH) (ab9485; Abcam) and α-tubulin (T9026; Sigma-Aldrich). Sources of other materials have been described elsewhere (39).

Cell culture. HUVECs and HAECs were propagated at 37°C in a humidified atmosphere containing 5% (vol/vol) CO_2 in ECM-2 medium (cambrex) supplemented with 2% (wt/vol) fetal bovine serum, hydrocortisone, ascorbate, and recombinant growth factors as recommended by the supplier. MEFs, 3T3 cells, and HEK293 cells were cultured in Dulbecco's modified Eagle's medium supplemented with 10% (vol/vol) fetal bovine serum, 1 mM L-glutamine, 100 U/ml penicillin, and 100 μg/ml streptomycin.

Transient transfection, siRNA, and morpholino delivery in HUVECs. Endotoxin-free cDNA expression constructs were prepared using a Wizard Purefection plasmid DNA purification system (Promega United Kingdom, Ltd., Southampton, United Kingdom). These were introduced into HUVECs by nucleofection per the manufacturer's instructions (Amaxa, Cologne, Germany). Briefly, 1×10^6 HUVECs per sample were resuspended in 100 μl of nucleofection buffer containing 1 μg of pMaxGFP (to assess transfection efficiency) and 4 μg of either pcDNA3 (vector control) or the desired construct indicated in the figures. Plasmid DNA was introduced into the nucleus of the cells using an Amaxa Nucleofector set at program U-O1. For antisense morpholino delivery, HUVECs plated in a six-well dish were incubated with 10 μM SOCS-3-specific antisense morpholino (5′-GAAACTTGCTGTGGGTGACCATG-3′) or a control morpholino against C/EBPα (5′-AGTTAGAGTTCTCCCGGCATGGCGA-3′), which is not expressed at detectable levels in these cells (data not shown), in combination with 6 μM Endo-Porter delivery reagent for 48 h prior to removal and subsequent experimental treatment. For introduction of siRNAs, 1×10^6 HUVECs/well plated in a six-well dish were treated twice over a period of 48 h using 20 μM siRNA oligonucleotides and 3 μl Oligofectamine as described by Kooistra et al. (26).

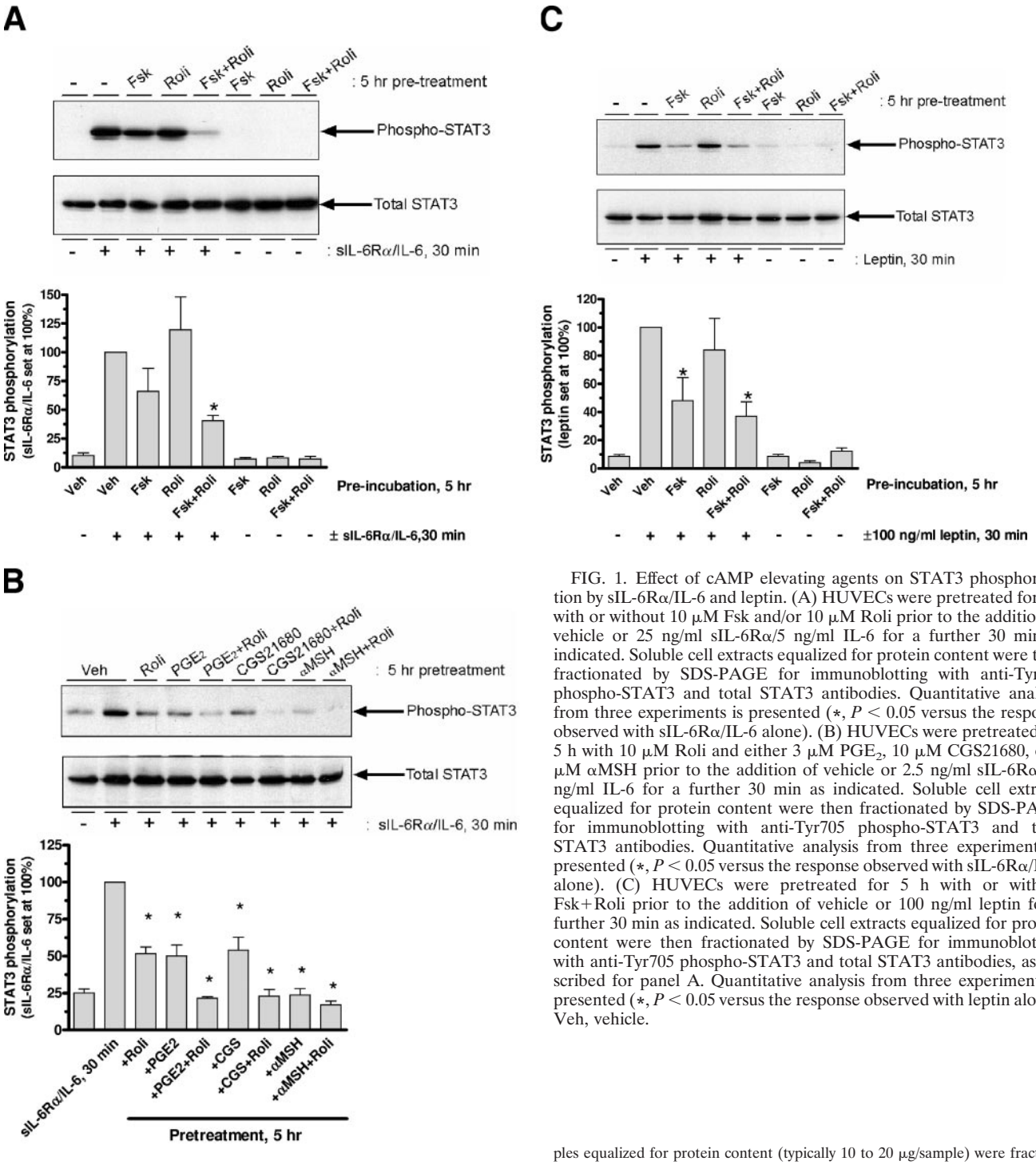

FIG. 1. Effect of cAMP elevating agents on STAT3 phosphorylation by sIL-6Rα/IL-6 and leptin. (A) HUVECs were pretreated for 5 h with or without 10 μM Fsk and/or 10 μM Roli prior to the addition of vehicle or 25 ng/ml sIL-6Rα/5 ng/ml IL-6 for a further 30 min as indicated. Soluble cell extracts equalized for protein content were then fractionated by SDS-PAGE for immunoblotting with anti-Tyr705 phospho-STAT3 and total STAT3 antibodies. Quantitative analysis from three experiments is presented (*, $P < 0.05$ versus the response observed with sIL-6Rα/IL-6 alone). (B) HUVECs were pretreated for 5 h with 10 μM Roli and either 3 μM PGE_2, 10 μM CGS21680, or 1 μM αMSH prior to the addition of vehicle or 2.5 ng/ml sIL-6Rα/0.5 ng/ml IL-6 for a further 30 min as indicated. Soluble cell extracts equalized for protein content were then fractionated by SDS-PAGE for immunoblotting with anti-Tyr705 phospho-STAT3 and total STAT3 antibodies. Quantitative analysis from three experiments is presented (*, $P < 0.05$ versus the response observed with sIL-6Rα/IL-6 alone). (C) HUVECs were pretreated for 5 h with or without Fsk+Roli prior to the addition of vehicle or 100 ng/ml leptin for a further 30 min as indicated. Soluble cell extracts equalized for protein content were then fractionated by SDS-PAGE for immunoblotting with anti-Tyr705 phospho-STAT3 and total STAT3 antibodies, as described for panel A. Quantitative analysis from three experiments is presented (*, $P < 0.05$ versus the response observed with leptin alone). Veh, vehicle.

Immunoblotting. Confluent cells in six-well plates were treated as described in the figure legends prior to washing in ice-cold phosphate-buffered saline (PBS) and solubilization by scraping into 50 μl/well detergent lysis buffer (50 mM sodium HEPES [pH 7.5], 150 mM sodium chloride, 5 mM EDTA, 10 mM sodium fluoride, 10 mM sodium phosphate, 1% [vol/vol] Triton X-100, 0.5% [wt/vol] sodium deoxycholate, 0.1% [wt/vol] sodium dodecyl sulfate [SDS], 0.1 mM phenylmethylsulfonyl fluoride, 10 μg/ml soybean trypsin inhibitor, 10 μg/ml benzamidine, and EDTA-free complete protease inhibitor mix). Following brief vortexing, insoluble material was removed by microcentrifugation, and the supernatant was assayed for protein content using a bicinchonic acid assay. Samples equalized for protein content (typically 10 to 20 μg/sample) were fractionated by SDS-polyacrylamide gel electrophoresis (PAGE) on 10 or 12% (wt/vol) resolving gels. Following transfer to nitrocellulose, membranes were blocked for 1 h at room temperature in blocking solution (5% [wt/vol] skim milk in PBS containing 0.1% [vol/vol] Tween 20). Membranes were then incubated either overnight at 4°C or for 1 h at room temperature with primary antibody diluted in fresh blocking buffer. Primary antibodies were each used at used at a final concentration of 1 μg/ml. Following three washes in blocking solution, membranes were incubated for 1 h at room temperature with appropriate horseradish peroxidase-conjugated secondary antibody at a 1-in-1,000 dilution. After further washes with blocking buffer and PBS, immunoreactive proteins were visualized by enhanced chemiluminescence. For phosphospecific antibodies, a similar protocol was used except that the primary antibodies were diluted in Tris-buffered

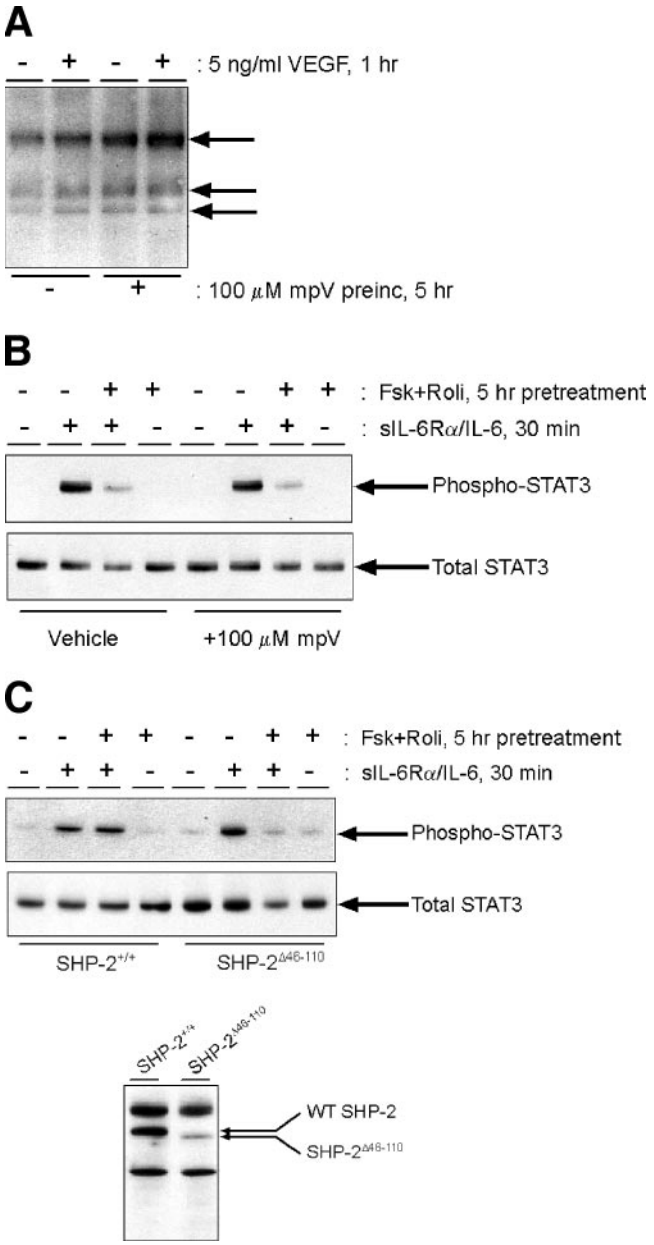

FIG. 2. Effect of SHP-2 inhibition on cAMP-mediated inhibition of STAT3 phosphorylation by sIL-6Rα/IL-6. (A) HUVECs were incubated with or without the protein Tyr phosphatase inhibitor mpV (100 μM) for 5 h prior to treatment with or without 5 ng/ml vascular endothelial growth factor (VEGF) for 1 h as indicated. Soluble cell extracts equalized for protein content were then fractionated by SDS-PAGE for immunoblotting with anti-phospho-Tyr antibody. The three most prominent immunoreactive bands are indicated. preinc, preincubation. (B) HUVECs were incubated with or without the protein Tyr phosphatase inhibitor mpV (100 μM) for 30 min prior to treatment with or without Fsk+Roli for 5 h and vehicle or 25 ng/ml sIL-6Rα/5 ng/ml IL-6 for a further 30 min as indicated. Soluble cell extracts equalized for protein content were then fractionated by SDS-PAGE for immunoblotting with anti-Tyr705 phospho-STAT3, total STAT3, and SOCS-3 antibodies. (C) Upper panels, SHP-$2^{+/+}$ and SHP-$2^{\Delta 46\text{-}110}$ 3T3 fibroblasts were pretreated with or without Fsk+Roli for 5 h prior to the addition of vehicle or sIL-6Rα/IL-6 for a further 30 min as shown in panel B. Soluble cell extracts equalized for protein content were then fractionated by SDS-PAGE for immunoblotting with anti-Tyr705 phospho-STAT3 and total STAT3 antibodies. Lower panel, lysates from SHP-$2^{+/+}$ and SHP-$2^{\Delta 46\text{-}110}$ 3T3 fibroblasts were also immunoblotted with anti-SHP-2 antibody to identify wild-type (WT) and mutated SHP-2 $^{\Delta 46\text{-}110}$, which migrates with enhanced mobility on SDS-PAGE due to the introduced deletion.

saline, pH 7.5, containing 5% (wt/vol) immunoglobulin G-free bovine serum albumin and 0.1% (vol/vol) Tween 20, and all washes were with Tris-buffered saline/0.1% (vol/vol) Tween 20. Quantification was by densitometric scanning of nonsaturating exposed films using TotalLab imaging software (Phoretix).

Quantitative reverse transcription-PCR analysis of SOCS-3 mRNA. Total RNA was isolated from stimulated HUVECs using TRIzol reagent. Two micrograms/sample was then utilized for cDNA synthesis using oligo(dT) primers in combination with avian myoblastosis virus reverse transcriptase (Promega, Southampton, United Kingdom) in accordance with the manufacturer's instructions. The cDNA for SOCS-3 was amplified and quantified using DyNAmo SYBR Green qPCR reagents (Finnzymes, Braintree, United Kingdom) using the forward primer 5′-CTTCAGCTCCAAGAGCGAGT-3′ and reverse primer 5′-CAGGTTCTTGGTCCCAGACT-3′, which generated a predicted 208-bp product, as verified by agarose gel electrophoresis. PCRs (25 μl, final volume) were performed in quadruplicate using a DNA Engine Opticon II real-time two-color PCR detection system (Bio-Rad Laboratories, Hemel Hempstead, United Kingdom) and employed 36 cycles of denaturation at 94°C (30 s), annealing at 50°C (20 s), and extension at 72°C (10 s). Melting curves were determined using the following parameters: 95°C cooling to 70°C, and ramping to 90°C at 0.2°C/s. Known amounts of pcDNA3/human SOCS-3 cDNA (0.1 fg to 1 ng) were amplified in parallel to allow quantification of the copy number from which inductions (*n*-fold) over basal levels were determined.

Sandwich ELISA for MCP-1. HUVECs in 96-well culture plates (10^4 cells/well) were treated in triplicate as indicated in Results. Aliquots of medium from each well were then assayed for MCP-1 accumulation using a sandwich ELISA kit in accordance with the manufacturer's instructions.

Statistical analysis. Data are presented in the text as means ± standard errors for the number of experiments indicated, while representative experiments are shown in the figures. Statistical significance was assessed by analysis of variance with an α probability of 0.05.

RESULTS

Effect of cAMP elevation on cytokine receptor activation of the JAK-STAT pathway in HUVECs. The effects of IL-6 in ECs are mediated by interaction of sIL-6Rα/IL-6 complexes with gp130 dimers at the cell surface (30). This activates the JAK-STAT signaling pathway, which mediates many of the effects of IL-6 exposure on target gene expression and EC function (19, 37). Preliminary experiments revealed that a 30-min exposure to maximally effective concentrations of sIL-6Rα/IL-6 stimulated the tyrosine phosphorylation of STAT3 24- ± 6-fold ($P < 0.05$ versus the vehicle-treated control; $n = 3$). Thus, to assess the functional consequences of cAMP elevation on receptor function, the effects of forskolin (Fsk) and rolipram (Roli) pretreatment on sIL-6Rα/IL-6-stimulated phosphorylation of STAT3 were assessed. Fsk directly binds and activates adenylyl cyclase isoforms to increase cAMP synthesis, while Roli blocks cAMP degradation by inhibiting the PDE4 family of phosphodiesterases (6, 21). While Roli alone had no effect on optimal STAT3 phosphorylation, treatments with Fsk alone and with Fsk and Roli together (Fsk+Roli) produced a substantial inhibition of STAT3 phosphorylation in response to either sIL-6Rα/IL-6 (67% ± 9% inhibition by Fsk+Roli versus vehicle-pretreated controls; $P < 0.05$; $n = 3$) without altering total levels of STAT3 protein (Fig. 1A). Importantly, similar inhibitory effects on STAT3 phosphorylation in response to sIL-6Rα/IL-6 were observed upon activation of endogenous G protein-coupled receptors for PGE_2 (via EP_2 and EP_4 recep-

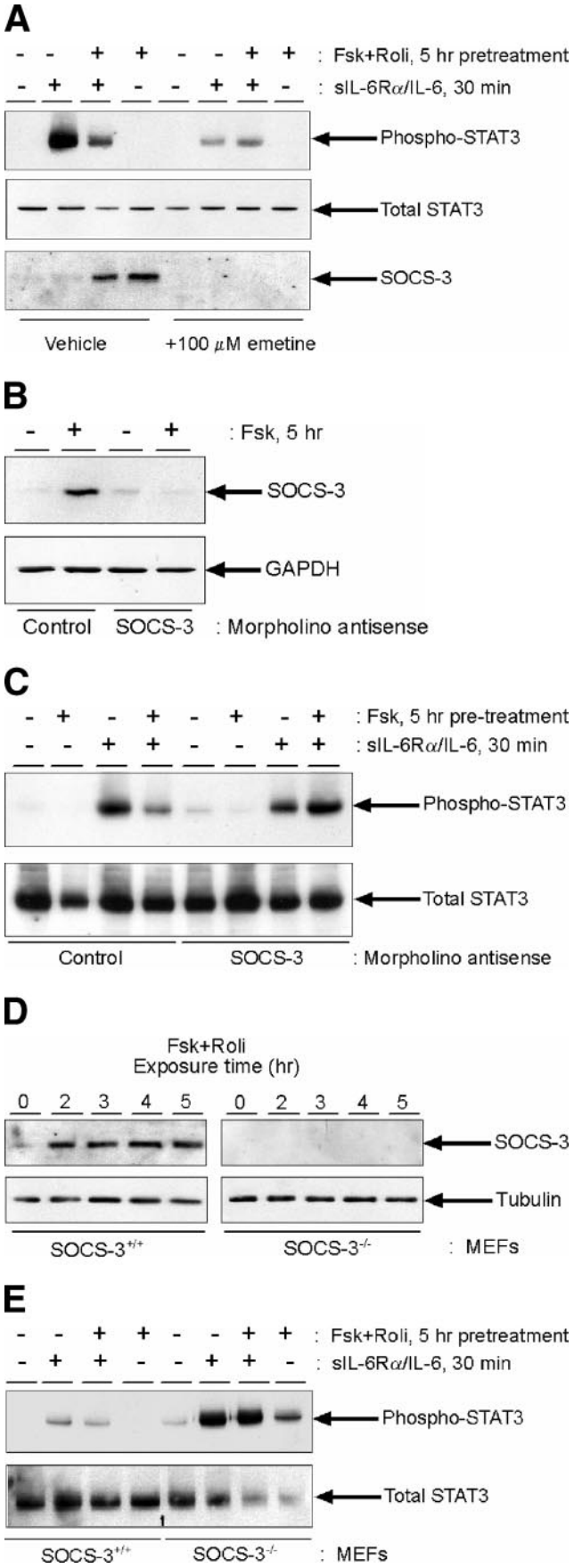

tors), CGS21680 (A_{2A} adenosine receptor [A_{2A}AR]) and αMSH (melanocortin receptor 1), each of which are known to activate adenylyl cyclase and elevate cAMP (11, 14, 33, 44) (Fig. 1B). In addition, the inhibitory effect of each agonist was potentiated by the inclusion of rolipram (Fig. 1B). To determine whether the effect of cAMP elevation was receptor specific, the effects of Fsk with or without Roli were also tested on STAT phosphorylation by leptin, which binds and activates the leptin receptor Ob-Rb in ECs (58). Leptin stimulated the tyrosine phosphorylation of STAT3 by 11- ± 1-fold ($P < 0.05$ versus the vehicle-treated control; $n = 3$) and, similar to the effect on sIL-6Rα/IL-6 responses, Fsk+Roli pretreatment inhibited this process (69% ± 15% inhibition versus vehicle-pretreated controls; $P < 0.05$; $n = 3$) without altering total levels of STAT3 protein (Fig. 1C). Thus, cAMP could significantly blunt the ability of both sIL-6Rα/IL-6 and leptin to activate the JAK-STAT pathway in vascular ECs.

Effects of blocking protein tyrosine phosphatase activity on cAMP-mediated inhibition of STAT3 phosphorylation. Several distinct molecular events serve to down-regulate class I cytokine receptor signaling (19). Since cAMP elevation specifically inhibited STAT3 phosphorylation in response to both sIL-6Rα/IL-6 and leptin without altering STAT3 expression, a common postreceptor inhibitory mechanism involving either protein tyrosine phosphatases, such as T-cell protein tyrosine phosphatase and SHP-2 and/or SOCS proteins, was likely to be operative (19, 58). With respect to the former possibility, it has been demonstrated by others that SHP-2 can be phosphorylated by PKA in vitro, resulting in an increase in its tyrosine phosphatase activity (35). Thus, to examine a role for tyrosine phosphatases in mediating the effects of cAMP, two distinct approaches were taken. First, HUVECs were pretreated with

FIG. 3. Effect of blocking SOCS-3 induction on cAMP-mediated inhibition of STAT3 phosphorylation by sIL-6Rα/IL-6. (A) HUVECs were incubated with or without the protein synthesis inhibitor emetine for 30 min prior to treatment with or without Fsk+Roli for 5 h and vehicle or 25 ng/ml sIL-6Rα and 5 ng/ml IL-6 for a further 30 min as indicated. Soluble cell extracts equalized for protein content were then fractionated by SDS-PAGE for immunoblotting with anti-Tyr705 phospho-STAT3, total STAT3, and SOCS-3 antibodies. (B) HUVECs were treated with SOCS-3 morpholino antisense oligonucleotide or a control morpholino for 48 h prior to treatment with or without 10 μM Fsk for 5 h as indicated and preparation of soluble cell extracts. Following equalization for protein content, samples were fractionated by SDS-PAGE for immunoblotting with anti-SOCS-3 and anti-GAPDH antibodies, the latter serving as a loading control. (C) HUVECs were treated with SOCS-3 morpholino antisense oligonucleotide or a control morpholino for 48 h prior to pretreatment with or without 10 μM Fsk for 5 h prior to the addition of vehicle or 25 ng/ml sIL-6Rα/5 ng/ml IL-6 for a further 30 min as indicated. Soluble cell extracts equalized for protein content were then fractionated by SDS-PAGE for immunoblotting with anti-Tyr705 phospho-STAT3 and total STAT3 antibodies. (D) SOCS-$3^{+/+}$ and SOCS-$3^{-/-}$ MEFs were treated with Fsk+Roli for the indicated times prior to the preparation of soluble cell extracts. Following equalization for protein content, samples were fractionated by SDS-PAGE for immunoblotting with anti-SOCS-3 and anti-tubulin antibodies, the latter serving as a loading control. (E) SOCS-$3^{+/+}$ and SOCS-$3^{-/-}$ MEFs were pretreated with or without Fsk+Roli for 5 h prior to the addition of vehicle or 25 ng/ml sIL-6Rα/5 ng/ml IL-6 for a further 30 min as indicated. Soluble cell extracts equalized for protein content were then fractionated by SDS-PAGE for immunoblotting with anti-Tyr705 phospho-STAT3 and total STAT3 antibodies.

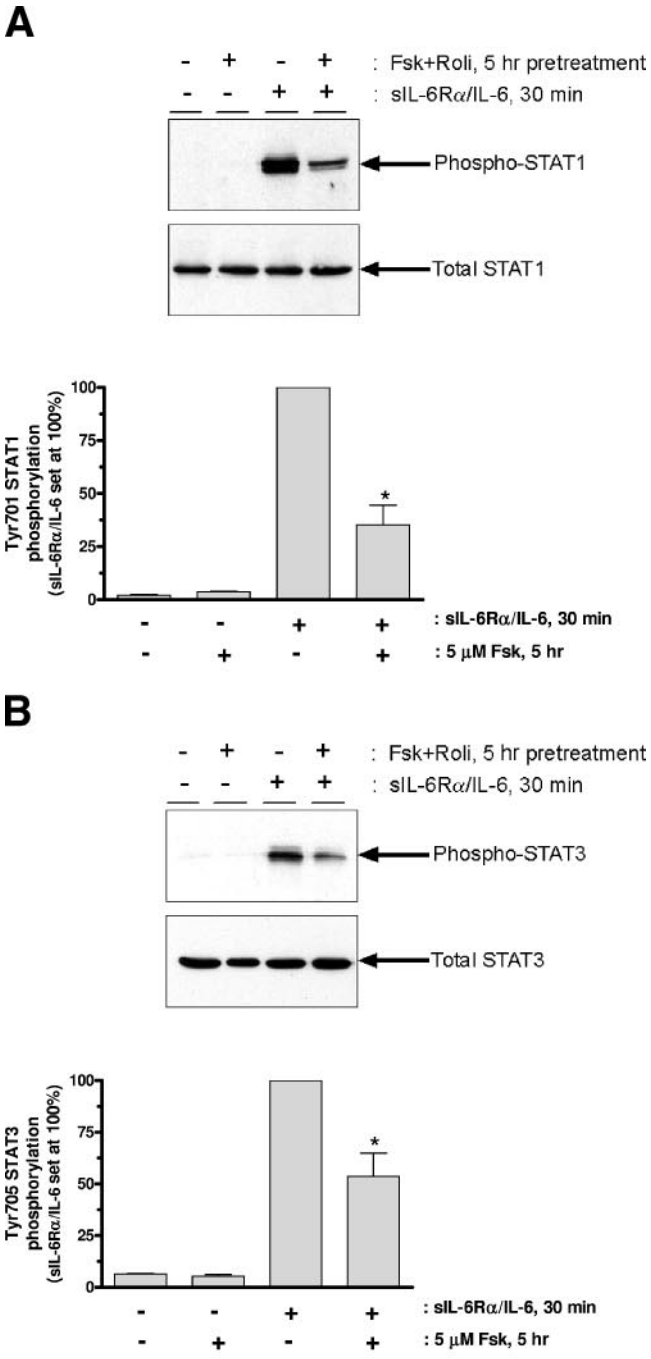

the protein tyrosine phosphatase inhibitor mpV prior to Fsk+Roli exposure and assessment of sIL-6Rα/IL-6-stimulated phosphorylation of STAT3. At a concentration (100 μM) at which mpV was effective in potentiating basal levels and vascular endothelial growth factor-stimulated increases in the Tyr phosphorylation of multiple intracellular proteins (Fig. 2A), no significant alteration in the inhibitory effect of Fsk+Roli was detectable (Fig. 2B) (mpV potentiated the inhibitory effect of Fsk+Roli by 34% ± 44%; $n = 3$; $P > 0.05$ [not significant {NS}]). In a second approach, experiments were also performed using SHP-$2^{+/+}$ and SHP-$2^{\Delta 46\text{-}110}$ 3T3 fibroblasts (59) to address a specific contribution of this tyrosine phosphatase in mediating the effects of cAMP. Interestingly in SHP-$2^{+/+}$ cells, no significant inhibition of sIL-6Rα/IL-6-stimulated STAT3 phosphorylation by Fsk+Roli was detectable. In contrast, the absence of functional SHP-2 in SHP-$2^{\Delta 46\text{-}110}$ cells was associated with a robust Fsk+Roli-mediated inhibition of STAT3 phosphorylation (Fig. 2B) (0% ± 10% inhibition in SHP-$2^{+/+}$ cells versus 77% ± 12% inhibition in SHP-$2^{\Delta 46\text{-}110}$ cells; $n = 3$; $P < 0.05$).

Effects of blocking SOCS-3 induction on cAMP-mediated inhibition of STAT3 phosphorylation. The expression of SOCS proteins is induced de novo upon cellular exposure to multiple stimuli (2, 27, 50, 51). Consequently, the inhibition of protein synthesis should exclude any contribution of SOCS induction toward mediating the effects of cAMP. Consistent with this hypothesis, the inhibition of protein synthesis by emetine pretreatment substantially reduced the ability of Fsk+Roli to inhibit sIL-6Rα/IL-6-stimulated phosphorylation of STAT3 (Fig. 3A) (100 μM emetine reduced the inhibitory effect of Fsk+Roli treatment by 61% ± 17%; $n = 4$; $P < 0.05$). We also noted that STAT3 phosphorylation by sIL-6Rα/IL-6 was reduced by emetine treatment in the absence of any change in total STAT3 levels, suggesting that the expression levels of JAKs and/or gp130 are reduced in the absence of any protein synthesis. This is consistent with observations that both gp130 and JAKs can be targeted for degradation in a cytokine-stimulated manner (3, 46). However, most importantly, parallel immunoblotting experiments demonstrated that Fsk+Roli treatment was capable of promoting the accumulation of SOCS-3 protein, an effect that was abolished by emetine pretreatment (Fig. 3A).

A specific role for SOCS-3 in mediating the inhibitory effects of cAMP was confirmed using two separate experimental approaches. The first involved using morpholino antisense oligo-

FIG. 4. Effect of cAMP elevation on SOCS-3 induction and STAT3 phosphorylation by sIL-6Rα/IL-6 in HAECs. HAECs were pretreated for 5 h with or without 10 μM forskolin prior to the addition of vehicle or 25 ng/ml sIL-6Rα and 5 ng/ml IL-6 for a further 30 min as indicated. Soluble cell extracts equalized for protein content were then fractionated by SDS-PAGE for immunoblotting with either anti-Tyr701 phospho-STAT1 and total STAT1 antibodies (A) or anti-Tyr705 phospho-STAT3 and total STAT3 antibodies (B). Quantitative analysis from three experiments is presented (*, $P < 0.05$ versus the response observed with sIL-6Rα/IL-6 alone). (C) HAECs were pretreated for 5 h with 10 μM Fsk prior to the preparation of soluble cell extracts. Following equalization for protein content, samples were fractionated by SDS-PAGE for immunoblotting with anti-SOCS-3 and anti-GAPDH antibodies, with the latter serving as a loading control.

nucleotides to test the effect of selectively blocking SOCS-3 induction on inhibition of STAT phosphorylation by cAMP in HUVECs. Under conditions in which Fsk-mediated induction of SOCS-3 was abolished (Fig. 3B), the ability of Fsk to inhibit sIL-6Rα/IL-6-stimulated phosphorylation of STAT3 was almost completely attenuated (Fig. 3C) (70% ± 15% inhibition in control morpholino-treated versus 15% ± 17% inhibition in SOCS-3 morpholino-treated HUVECs; $n = 3$; $P < 0.05$). The second approach involved comparing the inhibitory effect of cAMP elevation in SOCS-$3^{+/+}$ and SOCS-$3^{-/-}$ MEFs. Interestingly, both basal and sIL-6Rα/IL-6-stimulated levels of phosphorylated STAT3 were elevated in SOCS-$3^{-/-}$ MEFs, suggesting that low-level basal expression of SOCS-3 may play a role in dampening STAT3 activation under unstimulated conditions. Importantly, however, cAMP elevation was capable of strongly increasing SOCS-3 expression and inhibiting sIL-6Rα/IL-6-stimulated phosphorylation of STAT3 in SOCS-$3^{+/+}$ cells (Fig. 3D and E). Both effects were abolished in SOCS-$3^{-/-}$ cells (Fig. 3D and E) (51% ± 20% inhibition in SOCS-$3^{+/+}$ MEFs versus 1% ± 8% inhibition in SOCS-$3^{-/-}$ MEFs; $n = 3$; $P < 0.05$).

Taken together, these experiments argue against a role for SHP-2 and other protein tyrosine phosphatases in mediating the inhibitory effects of cAMP elevation on STAT3 phosphorylation by sIL-6Rα/IL-6 and instead suggest that cAMP-mediated up-regulation of the inhibitory regulator SOCS-3 is the mechanism responsible for this effect.

Inhibition of STAT phosphorylation in aortic ECs. It has been well documented that ECs from different vascular origins can display considerable variation in their biochemical and immunological properties, although they exhibit many overlapping functions (1). Thus, it was important to determine whether cAMP-mediated induction of SOCS-3 and subsequent inhibition of STAT phosphorylation was a phenomenon unique to HUVECs. To achieve this, the presence of the cAMP/SOCS-3 inhibitory pathway in HAECs was also assessed (Fig. 4). These experiments demonstrated that a 5-h pretreatment with Fsk inhibited sIL-6Rα/IL-6-mediated STAT phosphorylation to an extent similar to that observed with HUVECs (Fig. 4A and B) (65% ± 13% inhibition of STAT1 phosphorylation and 46% ± 15% inhibition of STAT3 phosphorylation; $n = 3$; $P < 0.05$ versus vehicle-pretreated controls). Fsk treatment also promoted the accumulation of SOCS-3 under these conditions (Fig. 4C). Thus, the ability of cAMP to inhibit sIL-6Rα/IL-6-mediated STAT phosphorylation and induce SOCS-3 expression is a feature common to ECs from both venous and arterial origins.

Characterization of cAMP-mediated induction of SOCS-3 expression in HUVECs. Exposure to Fsk produced a time-dependent accumulation of SOCS-3 protein that peaked after 4 h, was sustained for at least 24 h, and was temporally preceded by a transient induction of SOCS-3 mRNA (Fig. 5A and B). Importantly, SOCS-3 accumulation was observed not only with Fsk but also upon activation of endogenous cAMP-mobilizing G protein-coupled A_{2A}ARs by the selective agonist CGS21680 (Fig. 5C). Moreover, the effect appeared to be restricted to SOCS-3, as no induction of the otherwise closely related protein SOCS-1 was detectable in response to either CGS21680, Fsk, or Fsk+Roli under conditions in which recombinant SOCS-1 was readily detectable (Fig. 5D).

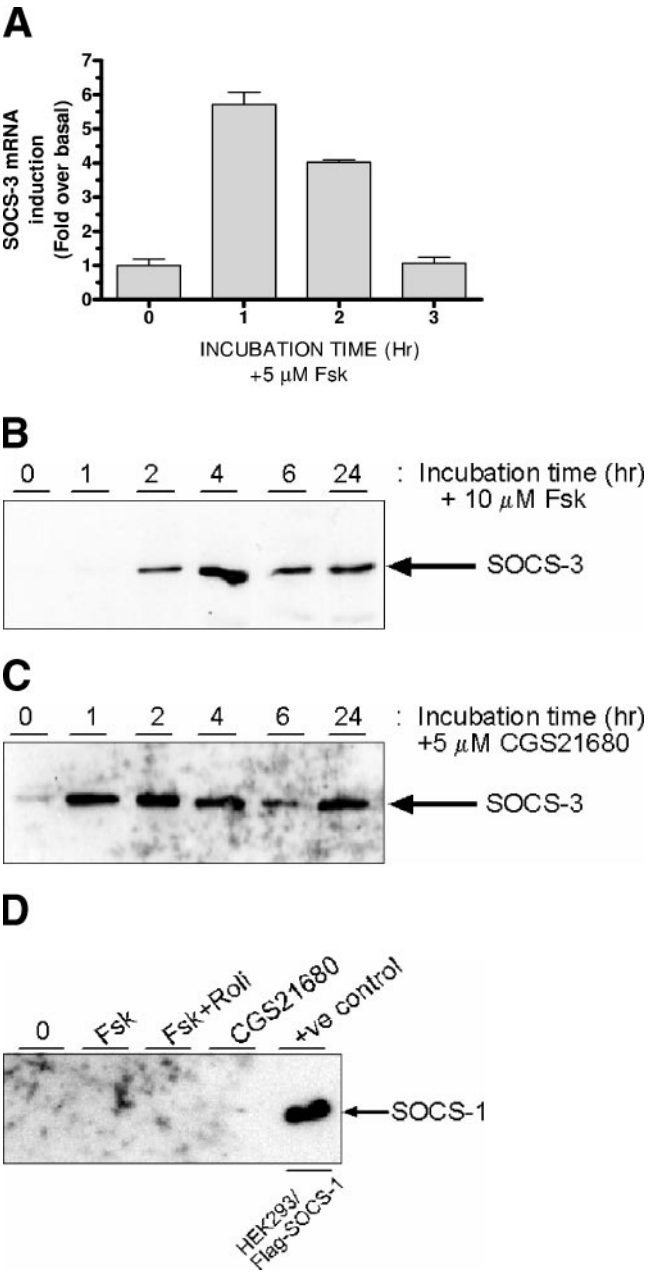

FIG. 5. Characterization of SOCS-3 induction following cAMP elevation in HUVECs. (A) HUVECs were treated with Fsk for the indicated times prior to the preparation of RNA and analysis of SOCS-3 mRNA by quantitative real-time reverse transcription-PCR. Results from one of four experiments is presented. (B) HUVECs were treated with Fsk for the indicated times prior to the preparation of soluble cell extracts. Following equalization for protein content, samples were fractionated by SDS-PAGE for immunoblotting with anti-SOCS-3 antibody. (C) HUVECs were treated with the A_{2A}AR-selective agonist CGS21680 (5 μM) for the indicated times prior to the preparation of soluble cell extracts. Following equalization for protein content, samples were fractionated by SDS-PAGE for immunoblotting with anti-SOCS-3 antibody. (D) HUVECs were treated with or without Fsk, Fsk+Roli, and CGS21680 for 5 h prior to the preparation of soluble cell extracts. Following equalization for protein content, samples were fractionated by SDS-PAGE for immunoblotting with anti-SOCS-1 antibody. Soluble extract (10 μg) prepared from HEK293 cells transiently expressing Flag epitope-tagged SOCS-1 (HEK293/Flag-SOCS-1) was run in parallel as a positive control for antibody immunoreactivity (+ve).

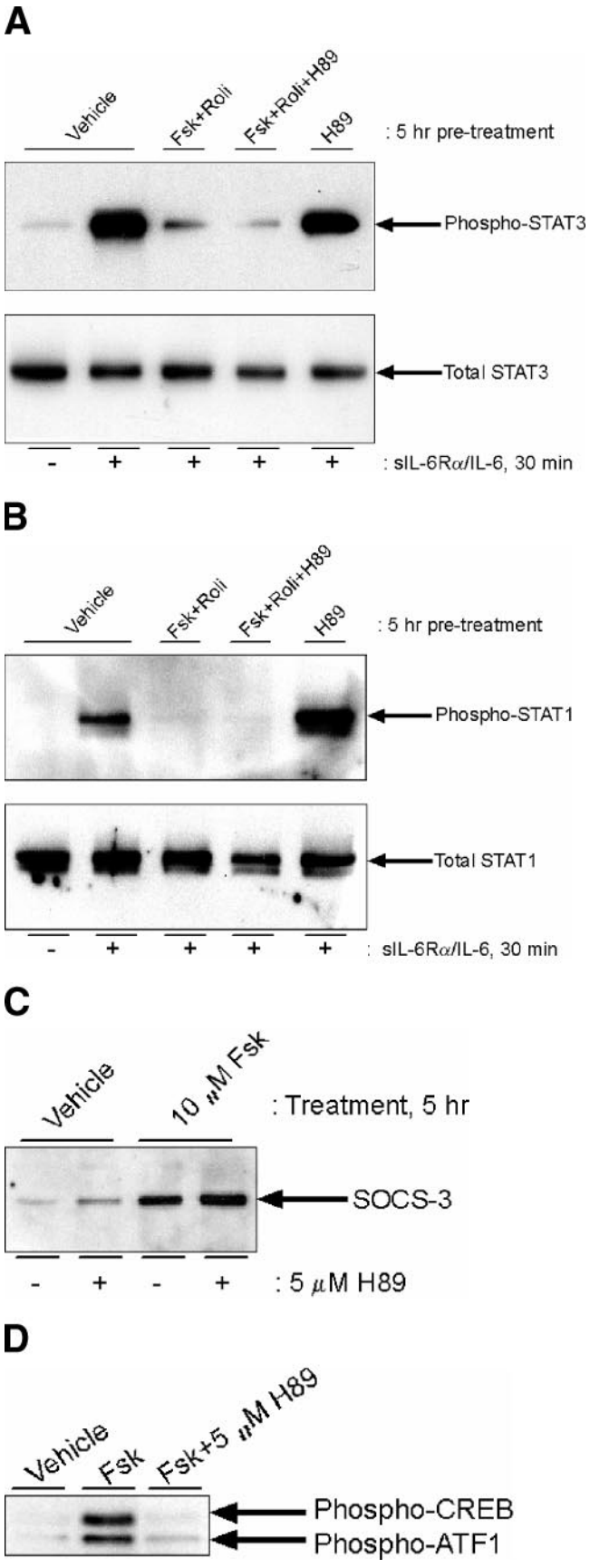

Effect of blocking PKA activity on SOCS-3 induction and inhibition of STAT phosphorylation. PKA is the most extensively characterized mediator of cAMP's intracellular effects (53) and thus represented an important potential effector of cAMP's inhibitory effects on STAT phosphorylation. However, under conditions in which pretreatment with Fsk+Roli substantially inhibited subsequent phosphorylation of STAT1 and STAT3 (77% ± 5% and 81% ± 4% inhibition, respectively, versus vehicle-pretreated controls; $P < 0.05$ for each; $n = 3$) (Fig. 6A and B), the effect could not be significantly reversed by coincubation with the PKA inhibitor H89 (7% ± 9% and 8% ± 5% reversal of STAT1 and STAT3 phosphorylation, respectively; $P > 0.05$ [NS]; $n = 3$) (Fig. 6A and B). Similarly, the ability of Fsk to promote the accumulation of SOCS-3 was not significantly inhibited by H89 pretreatment (2% ± 25% inhibition; $P > 0.05$ [NS]; $n = 3$) (Fig. 6C). These observations could not be explained by ineffective inhibition of PKA activity under these conditions, as the concentration of H89 employed (5 μM) abolished Fsk-stimulated PKA-mediated CREB phosphorylation on Ser133 (Fig. 6D). Thus, the ability of cAMP elevation to induce SOCS-3 and inhibit sIL-6Rα/IL-6-stimulated STAT phosphorylation occurs via a PKA-independent mechanism.

Contribution of Epac toward mediating SOCS-3 induction. The lack of any involvement of PKA in mediating cAMP's effect on SOCS-3 induction and inhibition of STAT phosphorylation suggested that alternative intracellular cAMP sensors were responsible. To test any contribution of Epac toward mediating these effects, the ability of the Epac-selective cAMP analogue 8-pCPT to induce SOCS-3 expression in HUVECs was initially tested. These experiments demonstrated that 8-pCPT could promote a concentration- and time-dependent accumulation of SOCS-3 (Fig. 7A and B). Epac functions as a guanine nucleotide exchange factor for the Rap family of small G proteins (5, 10). Thus, if Epac was involved in SOCS-3 induction, the activation of Rap should also be sufficient to trigger the effect. To test this hypothesis, the ability of constitutively active GTPase-deficient Val12Rap1a to promote the synthesis of SOCS-3 in HUVECs was assessed following transient expression over 48 h and pretreatment of cells with proteasome inhibitor MG132 to block SOCS-3 degradation by the proteasome at this time point. These experiments demon-

FIG. 6. Effect of blocking PKA activity on cAMP-mediated SOCS-3 induction and inhibition of STAT3 phosphorylation by sIL-6Rα/IL-6. HUVECs were incubated with or without the PKA inhibitor H89 (5 μM) for 30 min prior to treatment with Fsk+Roli for 5 h and vehicle or 25 ng/ml sIL-6Rα/5 ng/ml IL-6 for a further 30 min as indicated. Soluble cell extracts equalized for protein content were then fractionated by SDS-PAGE for immunoblotting with anti-Tyr705 phospho-STAT3 and total STAT3 (A) or anti-Tyr701 phospho-STAT1 and total STAT1 antibodies (B). (C) HUVECs were incubated with or without the PKA inhibitor H89 (5 μM) for 30 min prior to treatment with 10 μM Fsk for 5 h as indicated. Soluble cell extracts equalized for protein content were then fractionated by SDS-PAGE for immunoblotting with anti-SOCS-3 antibody. (D) HUVECs were incubated with or without the PKA inhibitor H89 (5 μM) for 30 min prior to treatment with 10 μM Fsk for 30 min as indicated. Soluble cell extracts equalized for protein content were then fractionated by SDS-PAGE for immunoblotting with anti-Ser133 phospho-CREB antibody.

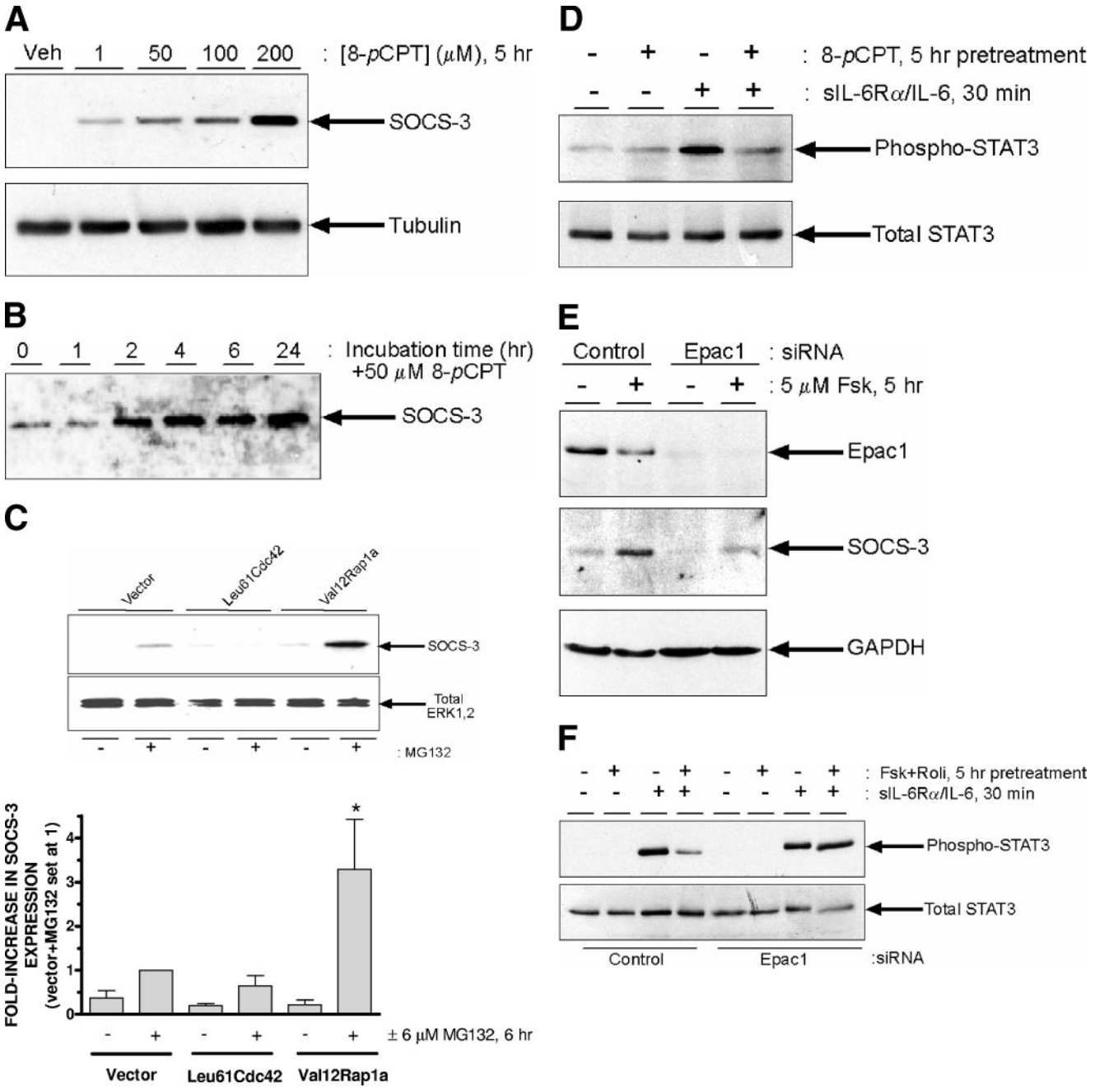

FIG. 7. Contribution of Epac toward SOCS-3 induction and inhibition of STAT3 phosphorylation by sIL-6Rα/IL-6. (A) HUVECs were treated with the indicated concentrations of the Epac-selective activator 8-pCPT for 5 h prior to the preparation of soluble cell extracts. Following equalization for protein content, samples were fractionated by SDS-PAGE for immunoblotting with anti-SOCS-3 and antitubulin antibodies, with the latter serving as a loading control. Veh, vehicle. (B) HUVECs were treated with 50 μM 8-pCPT for the indicated times prior to the preparation of soluble cell extracts. Following equalization for protein content, samples were fractionated by SDS-PAGE for immunoblotting with anti-SOCS-3 antibody. (C) HUVECs were transiently transfected with empty vector or expression constructs encoding Leu61Cdc42 and Val12Rap1a as indicated. Forty-eight hours posttransfection, cells were treated with or without 6 μM MG132 for 6 h prior to the preparation of soluble cell extracts. Following equalization for protein content, samples were then fractionated by SDS-PAGE for immunoblotting with anti-SOCS-3 and anti-ERK1/2 antibodies, with the latter serving as a loading control. Quantitative analysis from three experiments is presented (*, $P < 0.05$ versus the response observed with vector plus MG132). (D) HUVECs were pretreated for 5 h with or without 50 μM 8-pCPT prior to the addition of vehicle, 2.5 ng/ml sIL-6Rα, and 0.5 ng/ml IL-6 for a further 30 min as indicated. Soluble cell extracts equalized for protein content were then fractionated by SDS-PAGE for immunoblotting with anti-Tyr705 phospho-STAT3 and total STAT3 antibodies. (E) HUVECs were transfected twice over 48 h with nontargeting control and Epac1-specific siRNAs prior to treatment with Fsk for 5 h as indicated. Soluble cell extracts equalized for protein content were then fractionated by SDS-PAGE for immunoblotting with anti-Epac1, SOCS-3, and GAPDH antibodies. (F) HUVECs were transfected with control and Epac1-specific siRNAs as described for panel E prior to pretreatment with or without Fsk+Roli for 5 h followed by exposure to 25 ng/ml sIL-6Rα and 5 ng/ml IL-6 for 30 min as indicated. Soluble cell extracts equalized for protein content were then fractionated by SDS-PAGE for immunoblotting with anti-Tyr705 phospho-STAT3 and total STAT3 antibodies.

strated that expression of Val12Rap1a was sufficient to induce a 3.3- ± 1.5-fold increase in SOCS-3 levels over vector-transfected controls in the presence of proteasome inhibitor (Fig. 7C). In contrast, the expression of constitutively active Leu61-mutated Cdc42, a Rho family G protein, failed to increase SOCS-3 expression over vector controls (37% ± 30% inhibition of expression levels versus the vector-transfected control). To determine whether the increase in SOCS-3 expression induced by Epac was functionally relevant, we also tested the ability of 8-pCPT to inhibit STAT phosphorylation by sIL-6Rα/IL-6. Under these conditions, a 5-h pretreatment with 50 μM 8-pCPT caused an 81% ± 13% inhibition of STAT3 phosphorylation (Fig. 7D) ($P < 0.05$ versus vehicle-pretreated controls; $n = 3$). Together, these data demonstrate that selective activation of the Epac/Rap pathway is sufficient to recapitulate the ability of cAMP to induce the accumulation of SOCS-3 and inhibit sIL-6Rα/IL-6 signaling. To determine whether Epac activation was absolutely necessary to observe these effects, an siRNA strategy was used to specifically deplete cellular Epac1 expression (Epac2 is not expressed to a significant extent in HUVECs) (26). Under conditions where Epac1 expression was reduced by 87% ± 3%, the ability of Fsk+Roli to induce SOCS-3 was reduced by 61% ± 12% ($P < 0.05$ versus control cells; $n = 3$) (Fig. 7E), and inhibition of STAT3 phosphorylation was completely blocked (84% ± 13% inhibition in control cells versus −3% ± 21% inhibition in Epac1-depleted cells; $P < 0.05$ versus controls; $n = 3$) (Fig. 7F). Therefore, the presence of Epac1 is necessary and sufficient for cAMP elevation to induce SOCS-3 and thus inhibit sIL-6Rα/IL-6-mediated STAT3 phosphorylation.

Effect of Epac activation on sIL-6Rα/IL-6-stimulated accumulation of MCP-1. To assess the physiological significance of the cAMP/Epac/SOCS-3 pathway in inhibiting sIL-6Rα/IL-6-stimulated phosphorylation of STATs, it was important to determine whether cAMP elevation and Epac activation could suppress the induction of an important STAT-regulated gene product. Due to its key role as a chemoattractant responsible for leukocyte recruitment during the early stages of atherogenesis, the chemokine MCP-1 was chosen for analysis (37, 54). While exposure of HUVECs to a maximally effective concentration of sIL-6Rα/IL-6 produced a 5.2- ± 2.7-fold increase in MCP-1 accumulation after 24 h, pretreatment with Fsk+Roli for 5 h prior to sIL-6Rα/IL-6 exposure substantially inhibited MCP-1 release (Fig. 8). Importantly, this inhibition could be largely reproduced by the selective activation of Epac with 50 μM 8-pCPT (Fig. 8), a concentration at which SOCS-3 induction was readily detectable (Fig. 7A). Thus, Epac-mediated up-regulation of SOCS-3 represents an inhibitory mechanism capable of suppressing sIL-6Rα/IL-6-mediated up-regulation of an important STAT-responsive gene product involved in the progression of disease.

Identification of a cAMP-activated signaling pathway leading to SOCS-3 accumulation. One potentially trivial reason that SOCS-3 induction was observed in response to Fsk+Roli and 8-pCPT could have been contamination of these reagents with LPS, which has been shown to up-regulate multiple SOCS proteins in macrophages and HL60 cells (51). However, preincubation of each ligand with polymyxin B, which binds and inactivates LPS, failed to inhibit SOCS-3 induction (data not shown), thereby excluding the possibility that LPS contamination was responsible.

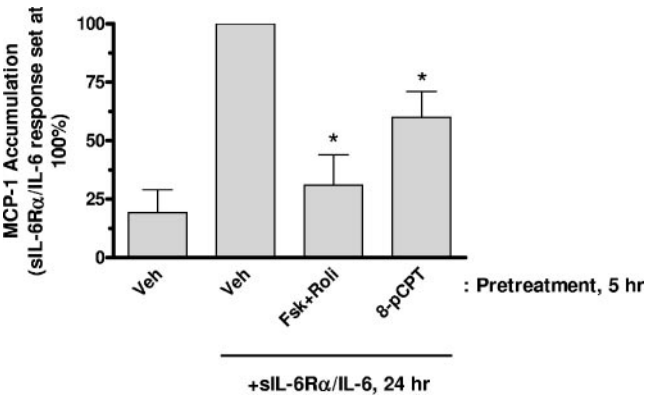

FIG. 8. Effect of Epac activation on the accumulation of MCP-1. HUVECs were pretreated with either vehicle (Veh), Fsk+Roli, or 50 μM 8-pCPT for 5 h prior to treatment with 25 ng/ml sIL-6Rα and 5 ng/ml IL-6 for 24 h as indicated. Conditioned medium was then removed for measurement of MCP-1 levels. Data from three experiments are presented (*, $P < 0.05$ versus sIL-6Rα/IL-6-stimulated MCP-1 levels). Basal MCP-1 levels were 0.69 ± 0.42 ng/ml ($n = 3$).

SOCS-3 induction in response to sIL-6Rα/IL-6 binding to gp130 is due to the activation of the JAK-STAT pathway and the subsequent binding of phosphorylated STAT dimers to a GAS element within the SOCS-3 promoter (18). Moreover, there is some evidence to suggest that G protein-coupled receptors, such as the thrombin receptor PAR-1 (28), are capable of directly activating the JAK-STAT pathway. Thus, to assess whether cAMP elevation triggered this pathway to up-regulate SOCS-3, the effects of JAK inhibition on Fsk+Roli- and sIL-6Rα/IL-6-mediated induction of SOCS-3 were compared. This demonstrated that while SOCS-3 induction in response to sIL-6Rα/IL-6 was essentially abolished by preincubation with a selective JAK inhibitor (96% ± 5% inhibition versus the vehicle-pretreated control; $P < 0.05$; $n = 3$), the response to Fsk+Roli remained largely intact (15% ± 12% inhibition versus the vehicle-pretreated control; $P > 0.05$ [NS]; $n = 3$) (Fig. 9A). Consistent with this observation, we have been unable to detect any Fsk+Roli stimulation of STAT1 or STAT3 tyrosine phosphorylation over a wide range of incubation times, spanning 15 min to 5 h (Fig. 1 to 3 and data not shown). Thus, cAMP elevation up-regulates SOCS-3 expression via a mechanism distinct from the JAK-dependent pathway utilized by sIL-6Rα/IL-6. However, Fsk-mediated induction of SOCS-3 was significantly reduced by preincubation with the MEK inhibitor U0126 (79% ± 16% inhibition versus the vehicle-pretreated control; $P < 0.05$; $n = 3$) (Fig. 9B). Indeed, the treatment of HUVECs with Fsk for 15 min produced a marked increase in ERK phosphorylation, equivalent to that produced by the protein kinase C activator phorbol 12-myristate 13-acetate (PMA) (45) (Fig. 9C). To determine whether ERK activation alone was sufficient to induce SOCS-3, we tested the ability of PMA treatment to induce SOCS-3. This demonstrated that PMA was able to induce SOCS-3 (6.6- ± 0.9-fold over the vehicle-treated control; $P < 0.05$; $n = 3$) and that induction was blocked by U0126, in contrast to the STAT-mediated induction of SOCS-3 produced by sIL-6Rα/IL-6,

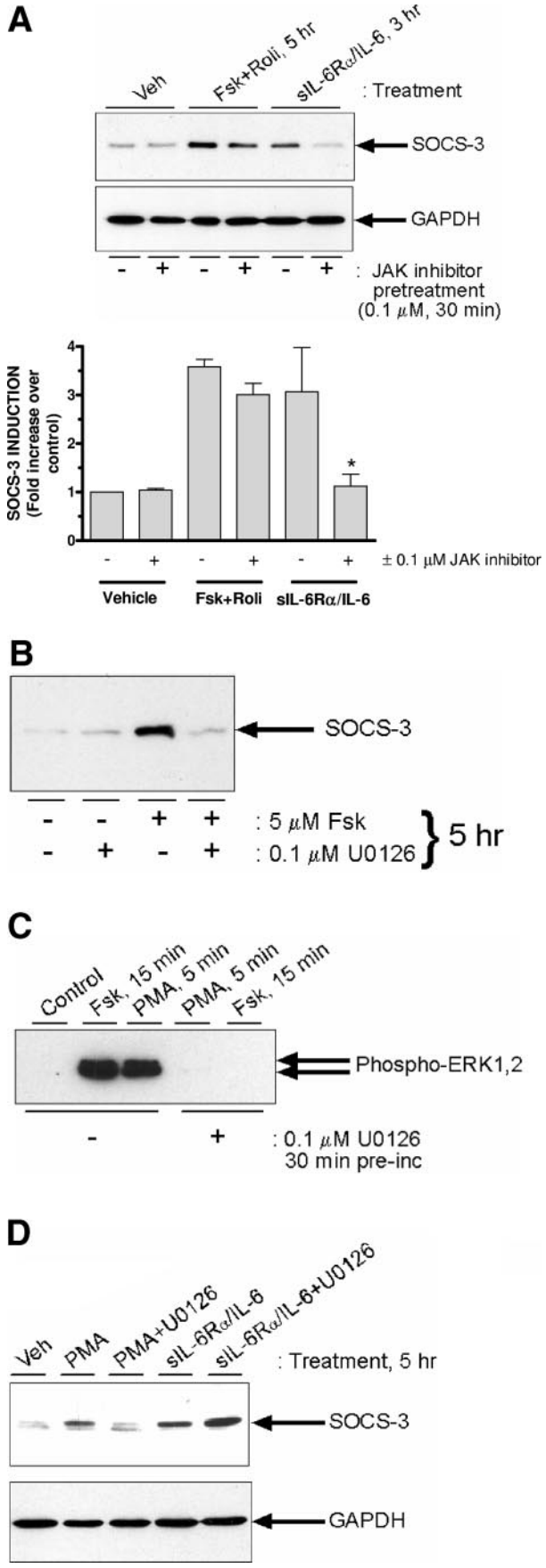

which was resistant to inhibition by U0126 (Fig. 9D). Thus, cAMP elevation in HUVECs can activate the ERK pathway, an event that appears to be sufficient to observe up-regulation of SOCS-3.

DISCUSSION

The prototypical second messenger cAMP occupies a central role in endothelial cell function by virtue of its ability to limit vascular permeability and attenuate pro-inflammatory events in response to multiple cytokines (4, 12, 15, 31). In this study, we have demonstrated that cAMP elevation can inhibit activation of the JAK-STAT pro-inflammatory signaling pathway in response to a sIL-6Rα/IL-6 *trans*-signaling complex by specifically promoting the accumulation of SOCS-3 via a novel PKA-independent mechanism that can be mimicked by activation of the recently identified cAMP sensor Epac. Although Epac was identified approximately 8 years ago, the biological effects it controls have only recently begun to emerge. These include positive regulation of integrin-mediated cell adhesion (11, 17), stimulation of insulin secretion via activation of ryanodine-sensitive calcium channels, and control of vesicle exocytosis (20, 24). Several studies have also recently identified a central role for Epac in controlling the ability of cAMP to reduce vascular permeability in part by potentiating the formation of VE-cadherin-mediated cell-cell interactions (9, 15, 26). Thus, our observation that Epac activation can stimulate the accumulation of SOCS-3, thereby resulting in an inhibition of gp130-mediated downstream signaling, is of interest from at least two perspectives. First, SOCS-3 induction represents a new function for Epac that is consistent with the predominantly anti-inflammatory effects of cAMP elevation observed for ECs (4). Second, our observations identify a second role for Epac in EC biology in addition to its effects on barrier function and would thus suggest that Epac is an especially important mediator of cAMP's effects in these cells. Therefore, selective manipulation of the cAMP-Epac-Rap pathway might prove to be a useful strategy for limiting multiple aspects of endothelial

FIG. 9. Identification of a signaling pathway controlling cAMP-mediated induction of SOCS-3. (A) HUVECs were pretreated for 30 min with or without 0.1 μM JAK inhibitor prior to the addition of either 25 ng/ml sIL-6Rα and 5 ng/ml IL-6 or Fsk+Roli for a further 3 or 5 h as indicated. Soluble cell extracts equalized for protein content were then fractionated by SDS-PAGE for immunoblotting with anti-SOCS-3 and anti-GAPDH antibodies, the latter serving as a loading control. Quantitative analysis from three experiments is presented (*, $P < 0.05$ versus sIL-6Rα/IL-6-stimulated SOCS-3 expression in the absence of JAK inhibitor). (B) HUVECs were pretreated for 30 min with or without MEK inhibitor U0126 (0.1 μM) prior to the addition of 5 μM Fsk for a further 5 h as indicated. Soluble cell extracts equalized for protein content were then fractionated by SDS-PAGE for immunoblotting with anti-SOCS-3 antibody. (C) HUVECs were pretreated with or without 0.1 μM U0126 prior to the addition of 5 μM Fsk or 1 μM PMA as indicated. Soluble cell extracts equalized for protein content were then fractionated by SDS-PAGE for immunoblotting with anti-Thr202/Tyr204 phospho-ERK1/2 antibody. (D) HUVECs were pretreated with or without 0.1 μM U0126 prior to the addition of 1 μM PMA or 25 ng/ml sIL-6Rα and 5 ng/ml IL-6 for 5 h as indicated. Soluble cell extracts equalized for protein content were then fractionated by SDS-PAGE for immunoblotting with anti-SOCS-3 and GAPDH antibodies. Veh, vehicle; pre-inc, preincubation.

dysfunction associated with disease. Interestingly, while others have observed that SHP-2 is positively regulated by cAMP via phosphorylation by PKA (35), we found that the ability of cAMP elevation to inhibit sIL-6Rα/IL-6 phosphorylation of STAT3 was markedly potentiated in cells expressing an SH2 domain-mutated SHP-$2^{\Delta 46\text{-}110}$. One explanation for this finding is that since the mutated SHP-2 in these cells is incapable of binding phospho-Tyr759 on activated gp130, more of this docking site is available for binding the SOCS-3 induced by cAMP elevation. It also suggests that cellular levels of SHP-2 may be an important determinant of the magnitude with which cAMP-mediated SOCS-3 induction can inhibit activation of the JAK-STAT pathway.

The ability of cAMP elevation to induce SOCS protein expression has been noted for other nonendothelial cell types, as evidenced by the strong induction we have observed with MEFs, and that others have noted with FRTL5 thyroid cells and neutrophils (16, 34). However, our study is the first to show that the induction of SOCS-3 is required for the inhibition of downstream signaling to occur and the first to define the novel PKA-independent molecular pathway responsible. Also, while cAMP has been reported to stimulate the accumulation of both SOCS-1 and SOCS-3 in FRTL-5 cells (34), we were unable to detect any accumulation of SOCS-1 in response to a panel of cAMP-elevating agents under conditions in which SOCS-3 induction was readily detectable, implying that cell type-specific differences may determine the pattern of SOCS isoform induction. Moreover, cAMP elevation increased Tyr705 phosphorylation of STAT3 in FRTL-5 cells (34), whereas the ability of cAMP to induce SOCS-3 in HUVECs is JAK independent and is not associated with any detectable increase in the Tyr phosphorylation of either STAT1 or STAT3. Thus, while the ability of cAMP elevation to promote the accumulation of SOCS proteins appears to be conserved between multiple cell types, the exact mechanisms involved may vary.

Interestingly, SOCS-3 accumulation in response to cAMP elevation in HUVECs was sustained for up to 24 h despite a transient increase in SOCS-3 mRNA being detectable only between 1 and 2 h (Fig. 5A and B). A similar transient appearance of SOCS-3 mRNA followed by sustained accumulation of SOCS-3 protein over 24 h has also been observed for HUVECs stimulated with oncostatin M which, like IL-6, signals via gp130 to activate the JAK-STAT pathway (29). In fact, we found destabilization of SOCS-3 only to be a major issue in Val12Rap1a transfection experiments (Fig. 7C), which were performed over a 48-h period and which necessitated the inclusion of MG132 to observe any reproducible accumulation of SOCS-3 protein. The sustained accumulation of SOCS-3 observed with endothelial cells contrasts with other cell types in which the accumulation of SOCS-3 is much more transient due to its rapid proteasomal degradation (40, 48). Degradation of SOCS-3 is triggered, at least in part, by phosphorylation of Tyr204 and/or -221 within the C-terminal SOCS box by either Src family kinases (SFKs) or JAKs (48). The related protein SOCS-1 is also sensitive to phosphorylation within its N-terminal region by the Ser/Thr kinases Pim1 and Pim2, which has the effect of stabilizing the protein (7). Finally, induction of an N-terminally truncated SOCS-3 due to alternative translation initiation at Met12, and thus rendered resistant to polyubquitylation and proteasomal degradation, is another potential mechanism by which sustained SOCS-3 protein levels could remain elevated (40). However, we found no evidence that cAMP elevation could promote the accumulation of detectable levels of truncated SOCS-3. Instead, it is more likely that SOCS-3 is subject to posttranslational modifications or protein-protein interactions within endothelial cells that limit either its phosphorylation by JAKs/SFKs or its degradation following phosphorylation. In this respect, other investigators have noted that the stability of SOCS-3 varies markedly in a cell type-specific manner (40), although the factors responsible for this variability remain uncharacterized.

Also of particular interest in our study is the observation that the activation of ERK appeared to be sufficient to observe SOCS-3 induction by cAMP. While the mechanism by which Ras triggers the ERK pathway via interaction with Raf kinases has been well characterized, the steps leading from Rap to ERK activation are controversial; some investigators have provided evidence for a positive interaction between GTP-bound Rap1 and B-Raf (57), while others have shown that the pathway can potentially be more indirect, involving sequential activation of a Rap2b/phospholipase C (PLC)-ε/RasGRP pathway leading to the accumulation of GTP-bound Ras (25). Rap1a is incapable of stimulating PLC-ε under conditions where Rap2b is active (13) and so, presumably, this pathway is not involved in SOCS-3 accumulation. It should also be noted that a sensitivity of SOCS-3 induction to inhibition of the ERK pathway does not necessarily exclude a contribution of other Epac-activated events in the control of SOCS-3 accumulation.

Cumulatively, our observations support the presence of a novel PKA-independent anti-inflammatory effect of cAMP elevation in vascular ECs that involves Epac-mediated accumulation of GTP-bound Rap1a, leading to the ERK-dependent up-regulation of SOCS-3, which then down-regulates receptor activation of the JAK-STAT pathway by sIL-6Rα/IL-6 and leptin. Further investigation will be required to identify the steps linking ERK activation to the accumulation of SOCS-3 transcript and to determine any significance of the Epac/SOCS-3 pathway in regulating the activity of other SOCS-3 binding partners, such as IRS1 (38, 49), that play critical roles in EC function in disease states (47).

ACKNOWLEDGMENTS

This work was supported by project grants from the British Heart Foundation, Heart Research UK, and the Biotechnology and Biological Sciences Research Council (to T.M.P.) and Ph.D. studentships from the British Heart Foundation (H.D.W.) and the UK Biotechnology and Biological Sciences Research Council (G.R.M.).

REFERENCES

1. **Aird, W. C.** 2005. Spatial and temporal dynamics of the endothelium. J. Thromb. Haemost. **3:**1392–1406.
2. **Alexander, W. S., and D. J. Hilton.** 2004. The role of suppressors of cytokine signaling (SOCS) proteins in regulation of the immune response. Annu. Rev. Immunol. **22:**503–529.
3. **Blanchard, F., W. Yanping, E. Kinzie, L. Duplomb, A. Godard, and H. Baumann.** 2001. Oncostatin M regulates the synthesis and turnover of gp130, leukemia inhibitory factor receptor α, and oncostatin M receptor-β by distinct mechanisms. J. Biol. Chem. **276:**47038–47045.
4. **Blease, K., A. Burke-Gaffney, and P. G. Hellewell.** 1998. Modulation of cell adhesion molecule expression and function on human lung microvascular endothelial cells by inhibition of phosphodiesterases 3 and 4. Br. J. Pharmacol. **124:**229–237.
5. **Bos, J. L.** 2003. Epac: a new cAMP target and new avenues in cAMP research. Nat. Rev. Mol. Cell Biol. **4:**733–738.
6. **Castro, A., M. J. Jerez, C. Gil, and A. Martinez.** 2005. Cyclic nucleotide

phosphodiesterases and their role in immunomodulatory responses: advances in the development of specific phosphodiesterase inhibitors. Med. Res. Rev. **25:**229–244.
7. **Chen, X. P., J. A. Losman, S. Cowan, E. Donahue, S. Fay, B. Q. Vuong, M. C. Nawijn, D. Capece, V. L. Cohan, and P. Rothman.** 2002. Pim serine/threonine kinases regulate the stability of Socs-1 protein. Proc. Natl. Acad. Sci. USA **99:**2175–2180.
8. **Croker, B. A., D. L. Krebs, J. G. Zhang, S. Wormald, T. A. Willson, E. G. Stanley, L. Robb, C. J. Greenhalgh, I. Forster, B. E. Clausen, N. A. Nicola, D. Metcalf, D. J. Hilton, A. W. Roberts, and W. S. Alexander.** 2003. SOCS3 negatively regulates IL-6 signaling in vivo. Nat. Immunol. **4:**540–545.
9. **Cullere, X., S. K. Shaw, L. Andersson, J. Hirahashi, F. W. Luscinskas, and T. N. Mayadas.** 2005. Regulation of vascular endothelial barrier function by Epac, a cAMP-activated exchange factor for Rap GTPase. Blood **105:**1950–1955.
10. **de Rooij, J., F. J. Zwartkruis, M. H. Verheijen, R. H. Cool, S. M. Nijman, A. Wittinghofer, and J. L. Bos.** 1998. Epac is a Rap1 guanine-nucleotide-exchange factor directly activated by cyclic AMP. Nature **396:**474–477.
11. **Dormond, O., M. Bezzi, A. Mariotti, and C. Ruegg.** 2002. Prostaglandin E_2 promotes integrin $\alpha_V\beta_3$-dependent endothelial cell adhesion, Rac-activation, and spreading through cAMP/PKA-dependent signaling. J. Biol. Chem. **277:**45838–45846.
12. **Enserink, J. M., L. S. Price, T. Methi, M. Mahic, A. Sonnenberg, J. L. Bos, and K. Tasken.** 2004. The cAMP-Epac-Rap1 pathway regulates cell spreading and cell adhesion to laminin-5 through the $\alpha_3\beta_1$ integrin but not the $\alpha_6\beta_4$ integrin. J. Biol. Chem. **279:**44889–44896.
13. **Evellin, S., J. Nolte, K. Tysack, F. vom Dorp, M. Thiel, P. A. Weernink, K. H. Jakobs, E. J. Webb, J. W. Lomasney, and M. Schmidt.** 2002. Stimulation of phospholipase C-ε by the M_3 muscarinic acetylcholine receptor mediated by cyclic AMP and the GTPase Rap2B. J. Biol. Chem. **277:**16805–16813.
14. **Feoktistov, I., S. Ryzhov, H. Zhong, A. E. Goldstein, A. Matafonov, D. Zeng, and I. Biaggioni.** 2004. Hypoxia modulates adenosine receptors in human endothelial and smooth muscle cells toward an A_{2B} angiogenic phenotype. Hypertension **44:**649–654.
15. **Fukuhara, S., A. Sakurai, H. Sano, A. Yamagishi, S. Somekawa, N. Takakura, Y. Saito, K. Kangawa, and N. Mochizuki.** 2005. Cyclic AMP potentiates vascular endothelial cadherin-mediated cell-cell contact to enhance endothelial barrier function through an Epac-Rap1 signaling pathway. Mol. Cell. Biol. **25:**136–146.
16. **Gasperini, S., L. Crepaldi, F. Calzetti, L. Gatto, C. Berlato, F. Bazzoni, A. Yoshimura, and M. A. Cassatella.** 2002. Interleukin-10 and cAMP-elevating agents cooperate to induce suppressor of cytokine signaling-3 via a protein kinase A-independent signal. Eur. Cytokine Netw. **13:**47–53.
17. **Gupta, M., and S. J. Yarwood.** 2005. MAP1A light chain 2 interacts with exchange protein activated by cyclic AMP 1 (EPAC1) to enhance Rap1 GTPase activity and cell adhesion. J. Biol. Chem. **280:**8109–8116.
18. **He, B., L. You, K. Uematsu, M. Matsangou, Z. Xu, M. He, F. McCormick, and D. M. Jablons.** 2003. Cloning and characterization of a functional promoter of the human SOCS-3 gene. Biochem. Biophys. Res. Commun. **301:**386–391.
19. **Heinrich, P. C., I. Behrmann, S. Haan, H. M. Hermanns, G. Muller-Newen, and F. Schaper.** 2003. Principles of interleukin (IL)-6-type cytokine signalling and its regulation. Biochem. J. **374:**1–20.
20. **Holz, G. G.** 2004. Epac: A new cAMP-binding protein in support of glucagon-like peptide-1 receptor-mediated signal transduction in the pancreatic β-cell. Diabetes **53:**5–13.
21. **Insel, P. A., and R. S. Ostrom.** 2003. Forskolin as a tool for examining adenylyl cyclase expression, regulation, and G protein signaling. Cell. Mol. Neurobiol. **23:**305–314.
22. **Jee, S. H., C. Y. Chu, H. C. Chiu, Y. L. Huang, W. L. Tsai, Y. H. Liao, and M. L. Kuo.** 2004. Interleukin-6 induced basic fibroblast growth factor-dependent angiogenesis in basal cell carcinoma cell line via JAK/STAT3 and PI3-kinase/Akt pathways. J. Investig. Dermatol. **123:**1169–1175.
23. **Kamizono, S., T. Hanada, H. Yasukawa, S. Minoguchi, R. Kato, M. Minoguchi, K. Hattori, S. Hatakeyama, M. Yada, S. Morita, T. Kitamura, H. Kato, K. I. Nakayama, and A. Yoshimura.** 2001. The SOCS box of SOCS-1 accelerates ubiquitin-dependent proteolysis of TEL-JAK2. J. Biol. Chem. **276:**12530–12538.
24. **Kang, G., J. W. Joseph, O. G. Chepurny, M. Monaco, M. B. Wheeler, J. L. Bos, F. Schwede, H. G. Genieser, and G. G. Holz.** 2003. Epac-selective cAMP analog 8-pCPT-2′-O-Me-cAMP as a stimulus for Ca^{2+}-induced Ca^{2+} release and exocytosis in pancreatic β-cells. J. Biol. Chem. **278:**8279–8285.
25. **Keiper, M., M. B. Stope, D. Szatkowski, A. Bohm, K. Tysack, F. Vom Dorp, O. Saur, P. A. Oude Weernink, S. Evellin, K. H. Jakobs, and M. Schmidt.** 2004. Epac- and Ca^{2+}-controlled activation of Ras and extracellular signal-regulated kinases by G_s-coupled receptors. J. Biol. Chem. **279:**46497–46508.
26. **Kooistra, M. R., M. Corada, E. Dejana, and J. L. Bos.** 2005. Epac1 regulates integrity of endothelial cell junctions through VE-cadherin. FEBS Lett. **579:**4966–4972.
27. **Kubo, M., T. Hanada, and A. Yoshimura.** 2003. Suppressors of cytokine signaling and immunity. Nat. Immunol. **4:**1169–1176.
28. **Madamanchi, N. R., S. Li, C. Patterson, and M. S. Runge.** 2001. Thrombin regulates vascular smooth muscle cell growth and heat shock proteins via the JAK-STAT pathway. J. Biol. Chem. **276:**18915–18924.
29. **Mahboubi, K., N. C. Kirkiles-Smith, J. Karras, and J. S. Pober.** 2002. Desensitization of signaling by oncostatin M in human vascular cells involves cytoplasmic Tyr residue 759 in gp130 but is not mediated by either Src homology 2 domain-containing tyrosine phosphatase 2 or suppressor of cytokine signaling 3. J. Biol. Chem. **278:**25014–25023.
30. **Marin, V., F. A. Montero-Julian, S. Gres, V. Boulay, P. Bongrand, C. Farnarier, and G. Kaplanski.** 2001. The IL-6-soluble IL-6Rα autocrine loop of endothelial activation as an intermediate between acute and chronic inflammation: an experimental model involving thrombin. J. Immunol. **167:**3435–3442.
31. **Morandini, R., G. Ghanem, A. Portier-Lemarie, B. Robaye, A. Renaud, and J. M. Boeynaems.** 1996. Action of cAMP on expression and release of adhesion molecules in human endothelial cells. Am. J. Physiol. **270:**H807–H816.
32. **Mori, H., R. Hanada, T. Hanada, D. Aki, R. Mashima, H. Nishinakamura, T. Torisu, K. R. Chien, H. Yasukawa, and A. Yoshimura.** 2004. SOCS3 deficiency in the brain elevates leptin sensitivity and confers resistance to diet-induced obesity. Nat. Med. **10:**739–743.
33. **Mountjoy, K. G., L. S. Robbins, M. T. Mortrud, and R. D. Cone.** 1992. The cloning of a family of genes that encode the melanocortin receptors. Science **257:**1248–1251.
34. **Park, E. S., H. Kim, J. M. Suh, S. J. Park, O. Y. Kwon, Y. K. Kim, H. K. Ro, B. Y. Cho, J. Chung, and M. Shong.** 2000. Thyrotropin induces SOCS-1 (suppressor of cytokine signaling-1) and SOCS-3 in FRTL-5 thyroid cells. Mol. Endocrinol. **14:**440–448.
35. **Rocchi, S., I. Gaillard, E. van Obberghen, E. M. Chambaz, and I. Vilgrain.** 2000. Adrenocorticotrophic hormone stimulates phosphotyrosine phosphatase SHP2 in bovine adrenocortical cells: phosphorylation and activation by cAMP-dependent protein kinase. Biochem. J. **352:**483–490.
36. **Rogers, R. S., C. M. Horvath, and M. J. Matunis.** 2003. SUMO modification of STAT1 and its role in PIAS-mediated inhibition of gene activation. J. Biol. Chem. **278:**30091–30097.
37. **Romano, M., M. Sironi, C. Toniatti, N. Polentarutti, P. Fruscella, P. Ghezzi, R. Faggioni, W. Luini, V. van Hinsbergh, S. Sozzani, F. Bussolino, V. Poli, G. Ciliberto, and A. Mantovani.** 1997. Role of IL-6 and its soluble receptor in induction of chemokines and leukocyte recruitment. Immunity **6:**315–325.
38. **Rui, L., M. Yuan, D. Frantz, S. Shoelson, and M. F. White.** 2002. SOCS-1 and SOCS-3 block insulin signaling by ubiquitin-mediated degradation of IRS1 and IRS2. J. Biol. Chem. **277:**42394–42398.
39. **Sands, W. A., A. F. Martin, E. W. Strong, and T. M. Palmer.** 2004. Specific inhibition of nuclear factor-κB-dependent inflammatory responses by cell type-specific mechanisms upon A_{2A} adenosine receptor gene transfer. Mol. Pharmacol. **66:**1147–1159.
40. **Sasaki, A., K. Inagaki-Ohara, T. Yoshida, A. Yamanaka, M. Sasaki, H. Yasukawa, A. E. Koromilas, and A. Yoshimura.** 2003. The N-terminal truncated isoform of SOCS3 translated from an alternative initiation AUG codon under stress conditions is stable due to the lack of a major ubiquitination site, Lys-6. J. Biol. Chem. **278:**2432–2436.
41. **Sasaki, A., H. Yasukawa, A. Suzuki, S. Kamizono, T. Syoda, I. Kinjyo, M. Sasaki, J. A. Johnston, and A. Yoshimura.** 1999. Cytokine-inducible SH2 protein-3 (CIS3/SOCS3) inhibits *Janus* tyrosine kinase by binding through the N-terminal kinase inhibitory region as well as SH2 domain. Genes Cells **4:**339–351.
42. **Schieffer, B., T. Selle, A. Hilfiker, D. Hilfiker-Kleiner, K. Grote, U. J. Tietge, C. Trautwein, M. Luchtefeld, C. Schmittkamp, S. Heeneman, M. J. Daemen, and H. Drexler.** 2004. Impact of interleukin-6 on plaque development and morphology in experimental atherosclerosis. Circulation **110:**3493–3500.
43. **Schmitz, J., M. Weissenbach, S. Haan, P. C. Heinrich, and F. Schaper.** 2000. SOCS3 exerts its inhibitory function on interleukin-6 signal transduction through the SHP2 recruitment site of gp130. J. Biol. Chem. **275:**12848–12856.
44. **Scholzen, T. E., C. Sunderkotter, D. H. Kalden, T. Brzoska, M. Fastrich, T. Fisbeck, C. A. Armstrong, J. C. Ansel, and T. A. Luger.** 2003. Alpha-melanocyte stimulating hormone prevents lipopolysaccharide-induced vasculitis by down-regulating endothelial cell adhesion molecule expression. Endocrinology **144:**360–370.
45. **Sexl, V., G. Mancusi, C. Holler, E. Gloria-Maercker, W. Schutz, and M. Freissmuth.** 1997. Stimulation of the mitogen-activated protein kinase via the A_{2A}-adenosine receptor in primary human endothelial cells. J. Biol. Chem. **272:**5792–5799.
46. **Shang, L., and T. B. Tomasi.** 2006. The heat shock protein 90-CDC37 chaperone complex is required for signaling by types I and II interferons. J. Biol. Chem. **281:**1876–1884.
47. **Sjoholm, A., and T. Nystrom.** 2005. Endothelial inflammation in insulin resistance. Lancet **365:**610–612.
48. **Sommer, U., C. Schmid, R. M. Sobota, U. Lehmann, N. J. Stevenson, J. A. Johnston, F. Schaper, P. C. Heinrich, and S. Haan.** 2005. Mechanisms of SOCS3 phosphorylation upon interleukin-6 stimulation: contributions of Src- and receptor-tyrosine kinases. J. Biol. Chem. **280:**31478–31488.

49. **Steppan, C. M., J. Wang, E. L. Whiteman, M. J. Birnbaum, and M. A. Lazar.** 2005. Activation of SOCS-3 by resistin. Mol. Cell. Biol. **25:**1569–1575.
50. **Stevenson, N. J., S. Haan, A. E. McClurg, M. J. McGrattan, M. A. Armstrong, P. C. Heinrich, and J. A. Johnston.** 2004. The chemoattractants, IL-8 and formyl-methionyl-leucyl-phenylalanine, regulate granulocyte colony-stimulating factor signaling by inducing suppressor of cytokine signaling-1 expression. J. Immunol. **173:**3243–3249.
51. **Stoiber, D., P. Kovarik, S. Cohney, J. A. Johnston, P. Steinlein, and T. Decker.** 1999. Lipopolysaccharide induces in macrophages the synthesis of the suppressor of cytokine signaling 3 and suppresses signal transduction in response to the activating factor IFN-γ. J. Immunol. **163:**2640–2647.
52. **Tanaka, T., M. A. Soriano, and M. J. Grusby.** 2005. SLIM is a nuclear ubiquitin E3 ligase that negatively regulates STAT signaling. Immunity **22:** 729–736.
53. **Tasken, K., and E. M. Aandahl.** 2004. Localized effects of cAMP mediated by distinct routes of protein kinase A. Physiol. Rev. **84:**137–167.
54. **Von der Thusen, J. H., J. Kuiper, T. J. van Berkel, and E. A. Biessen.** 2003. Interleukins in atherosclerosis: molecular pathways and therapeutic potential. Pharmacol. Rev. **55:**133–166.
55. **Wormald, S., and D. J. Hilton.** 2004. Inhibitors of cytokine signal transduction. J. Biol. Chem. **279:**821–824.
56. **Yasukawa, H., M. Ohishi, H. Mori, M. Murakami, T. Chinen, D. Aki, T. Hanada, K. Takeda, S. Akira, M. Hoshijima, T. Hirano, K. R. Chien, and A. Yoshimura.** 2003. IL-6 induces an anti-inflammatory response in the absence of SOCS3 in macrophages. Nat. Immunol. **4:**551–556.
57. **York, R. D., H. Yao, T. Dillon, C. L. Ellig, S. P. Eckert, E. W. McCleskey, and P. J. Stork.** 1998. Rap1 mediates sustained MAP kinase activation induced by nerve growth factor. Nature **392:**622–626.
58. **Zabeau, L., D. Lavens, F. Peelman, S. Eyckerman, J. Vandekerckhove, and J. Tavernier.** 2003. The ins and outs of leptin receptor activation. FEBS Lett. **546:**45–50.
59. **Zhang, S. Q., W. G. Tsiaras, T. Araki, G. Wen, L. Minichiello, R. Klein, and B. G. Neel.** 2002. Receptor-specific regulation of phosphatidylinositol 3′-kinase activation by the protein tyrosine phosphatase Shp2. Mol. Cell. Biol. **22:**4062–4072.